Valence states and occupation sites in $(Fe,Mn)_3O_4$ spinel oxides investigated by soft x-ray absorption spectroscopy and magnetic circular dichroism

2008 J. Phys.: Condens. Matter 20 295203

(http://iopscience.iop.org/0953-8984/20/29/295203)

J. Phys.: Condens. Matter **20** (2008) 295203 (5pp) doi:10.1088/0953-8984/20/29/295203

Valence states and occupation sites in $(Fe,Mn)_3O_4$ spinel oxides investigated by soft x-ray absorption spectroscopy and magnetic circular dichroism

H J Lee[1], G Kim[1], D H Kim[1], J-S Kang[1,6], C L Zhang[2], S-W Cheong[2], J H Shim[3], Soonchil Lee[3], Hangil Lee[4], J-Y Kim[4], B H Kim[5] and B I Min[5]

[1] Department of Physics, The Catholic University of Korea (CUK), Bucheon 420-743, Korea
[2] Rutgers Center for Emergent Materials and Department of Physics, Rutgers University, Piscataway, NJ 08854, USA
[3] Department of Physics, KAIST, Daejeon 305-701, Korea
[4] Pohang Accelerator Laboratory (PAL), POSTECH, Pohang 790-784, Korea
[5] Department of Physics, POSTECH, Pohang 790-784, Korea

E-mail: kangjs@catholic.ac.kr

Received 31 December 2007, in final form 23 March 2008
Published 26 June 2008
Online at stacks.iop.org/JPhysCM/20/295203

Abstract

The electronic structures of $(Fe,Mn)_3O_4$ spinel oxides have been investigated by employing soft-x-ray absorption spectroscopy (XAS) and soft x-ray magnetic circular dichroism (XMCD). We have determined the valence states as well as the occupation sites of Mn and Fe ions in $Fe_{0.9}Mn_{2.1}O_4$ and $MnFe_2O_4$. $Fe_{0.9}Mn_{2.1}O_4$ is found to be close to the inverse spinel (the inversion parameter $y \approx 0.85$), while $MnFe_2O_4$ is close to the normal spinel ($y \approx 0.2$). In $Fe_{0.9}Mn_{2.1}O_4$, Fe ions are mainly trivalent and the majority of Fe^{3+} ions occupy the octahedral B sites, while Mn ions are mixed-valent with approximately 45% Mn_A^{2+} at the tetrahedral A sites and 55% Mn_B^{3+} ions at the octahedral B sites. In $MnFe_2O_4$, Mn ions are mainly divalent and the majority of Mn^{2+} ions occupy the tetrahedral A sites, while Fe ions are mainly trivalent and the majority of Fe^{3+} ions occupy the octahedral B sites.

(Some figures in this article are in colour only in the electronic version)

1. Introduction

The AB_2O_4-type spinel oxides of $(M,M')_3O_4$ exhibit very interesting phenomena, such as the Jahn–Teller effect [1, 2] and phase separations [3]. When both M and M′ cations are magnetic ions, as in $MnFe_2O_4$, a ferrimagnetic ordering is often observed since the antiferromagnetic A–B interaction is dominating [4]. In MM'_2O_4 spinels, a cation occupies either the tetrahedral (T_d) A site or the octahedral (O_h) B site. Hence the MM'_2O_4 spinels are often described as $(M_{1-y}M'_y)_A[M'_{2-y}M_y]_BO_4$, where y is called the inversion parameter. The cases of $y = 0$ and 1 are called as the normal and inverse spinels, respectively. In $(M,M')_3O_4$-type spinel oxides with transition-metal elements [5], such as M, M′ = Co, Fe, Mn, it is widely believed that A site ions are divalent and that B site ions are trivalent. However, there are some controversies about the valence and spin states of M and M′ ions [6–13]. For example, in $(Fe,Fe)_3O_4$ magnetite, Fe ions at A sites are known to be trivalent, while Fe ions at B sites are in the Fe^{2+}–Fe^{3+} mixed-valent states. In contrast, for the valence states of Mn and Fe ions in $MnFe_2O_4$, no consensus has been reached yet. It was once proposed [6] that the valence states of Mn and Fe ions are mixed-valent such that $(Mn^{2+}_{1-y}Fe^{3+}_y)_A[Fe^{3+}_{2-2y}Fe^{2+}_yMn^{3+}_y]_BO_4$. However, Mössbauer measurements [8] and nuclear magnetic resonance (NMR) measurements [12, 14, 15] were analyzed to produce

[6] Author to whom any correspondence should be addressed.

different results: the single-valent states of Mn^{2+} and Fe^{3+} from the former, while the mixed-valent states of Mn^{2+}–Mn^{3+} and Fe^{2+}–Fe^{3+} from the latter. Therefore it is important to determine the valence states and spin structures of M and M′ ions in $(M,M')_3O_4$ microscopically.

Soft x-ray absorption spectroscopy (XAS) and soft x-ray magnetic circular dichroism (XMCD) are powerful experimental tools for studying the valence states and the local symmetries of T ions [16–18], and the element-specific local magnetic moments of spin and orbital components [19–21], respectively. The magnitudes of the spin moment (m_s) and the orbital moment (m_l) can be estimated quantitatively by applying the sum rules to the measured XMCD spectrum [19, 20]. In this paper, by employing XAS and XMCD, we have investigated the electronic structures of $(Fe,Mn)_3O_4$: $Fe_{0.9}Mn_{2.1}O_4$ (FMO) and $MnFe_2O_4$. $MnFe_2O_4$ is one of the prototype ferrimagnetic spinel oxides, and there are a few previous studies available [10, 22]. For FMO spinel, however, this is the first work that reports its electronic structure. We have determined the valence states of Mn and Fe ions and the occupation sites of Mn and Fe ions in $(Fe,Mn)_3O_4$.

2. Experimental details

FMO exhibits a phase separation depending on the annealing conditions in the growth process [3]. FMO single crystal, employed in this study, does not show any phase separation. The details of the sample growth will be described elsewhere [23]. The $MnFe_2O_4$ sample is the commercially available polycrystalline powder of 99.9% purity synthesized by KOJUNDO Chemical[7]. XRD measurements showed the sharp peaks that are characteristic of the single-phase *bulk* spinel structure. XAS and XMCD experiments were performed at the 2A undulator beamline of the PAL. The 2A beamline is an elliptically polarized undulator, from which the circularly polarized light was obtained with the degree of circular polarization of >90%. The XMCD spectra were taken for a fixed helicity of light by reversing the applied magnetic field at each $h\nu$. In order to minimize the artificial effects caused by the decreasing photon flux with time, the direction of the applied magnetic field was reversed at each data point in the XMCD data acquisition. The FMO single crystal was cleaved *in situ*, and XAS and XMCD data were collected in the total electron yield (TEY) mode[8]. XMCD spectra were obtained under the applied magnetic field of ∼0.7 T. $MnFe_2O_4$ was measured at $T \sim 80$ K, while the FMO crystal was measured at room temperature due to charging at low temperature. The total resolution for XAS was less than 100 meV, while that for XMCD was ∼120 meV at the Mn and Fe 2p absorption edges.

3. Results and discussion

Figure 1(a) shows the measured Fe 2p XAS spectra of $(Fe,Mn)_3O_4$. As a guide of the valence states of Fe ions, reference Fe 2p XAS spectra are shown below:

[7] SEM (scanning electron microscope) measurements showed that the average grain size of the $MnFe_2O_4$ sample is larger than a few μm.

[8] The TEY mode has a proving depth of 50–100 Å.

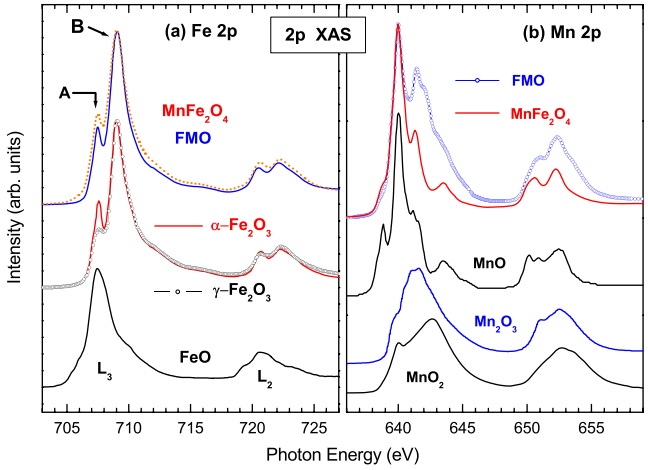

Figure 1. (a) Comparison of the Fe 2p XAS of $(Fe,Mn)_3O_4$ to those of α-Fe_2O_3, γ-Fe_2O_3 and FeO. (b) Comparison of the Mn 2p XAS spectra of $(Fe,Mn)_3O_4$ to those of MnO (Mn^{2+}), Mn_2O_3 (Mn^{3+}) and MnO_2 (Mn^{4+}).

α-Fe_2O_3 [24, 25] and γ-Fe_2O_3 [24] both as formally trivalent Fe^{3+} oxides ($3d^5$) but having different local symmetries, and FeO [25] as a formally divalent Fe^{2+} oxide ($3d^6$). The Fe 2p XAS spectra of $(Fe,Mn)_3O_4$ are very similar to those of both α-Fe_2O_3 and γ-Fe_2O_3, but quite different from that of FeO, indicating that the valence states of Fe ions in $(Fe,Mn)_3O_4$ are mainly trivalent (3+). Note that the intensity of the peak 'A' with respect to that of the peak 'B' decreases from α-Fe_2O_3 to $(Fe,Mn)_3O_4$ and γ-Fe_2O_3. All Fe^{3+} ions in α-Fe_2O_3 have the O_h sites only, while γ-Fe_2O_3 is often represented by $Fe^{3+}_A[Fe^{3+}_{5/3}V_{1/3}]_BO_4$ spinel with vacancies (V) at B sites. Hence Fe^{3+} ions in γ-Fe_2O_3 have both the T_d and O_h sites. Then the lower intensity of A/B in $(Fe,Mn)_3O_4$, than in α-Fe_2O_3, suggests the existence of Fe^{3+} ions at the T_d sites. In other words, Fe ions in $(Fe,Mn)_3O_4$ occupy both B(O_h) and A(T_d) sites. Further, the lower intensity of A/B in FMO than in $MnFe_2O_4$ reflects that more Fe ions occupy A(T_d) sites in FMO. This conclusion will be confirmed later in figure 4.

Similarly, figure 1(b) compares the measured Mn 2p XAS spectra of $(Fe,Mn)_3O_4$ to those of reference Mn systems of MnO (Mn^{2+}) [27], Mn_2O_3 (Mn^{3+}) [28] and MnO_2 (Mn^{4+}) [27]. The Mn 2p XAS spectrum of $MnFe_2O_4$ is qualitatively similar to that of MnO, but quite different from those of Mn_2O_3 and MnO_2, suggesting that Mn ions in $MnFe_2O_4$ are nearly divalent. In contrast, the features in FMO resemble those of both MnO and Mn_2O_3, suggesting that Mn ions are in the Mn^{2+}–Mn^{3+} mixed-valent states.

Figure 2 compares the measured Fe 2p XAS spectra of $(Fe,Mn)_3O_4$ to the calculated Fe 2p XAS spectra, obtained from the ligand field multiplet (LFM) model calculations [17] by including the spin–orbit (LS) interaction between 3d electrons. The three calculated XAS spectra (blue lines) represent those for Fe^{3+}_B ($3d^5$; O_h) with $10Dq = 1.5$ eV, Fe^{3+}_A ($3d^5$; T_d) with $10Dq = 1.2$ eV and Fe^{2+}_B ($3d^6$; O_h) with $10Dq = 1.5$ eV, respectively. It appears that the observed features in the measured Fe 2p XAS spectra in $(Fe,Mn)_3O_4$ are described better by the calculated Fe^{3+} states than by the

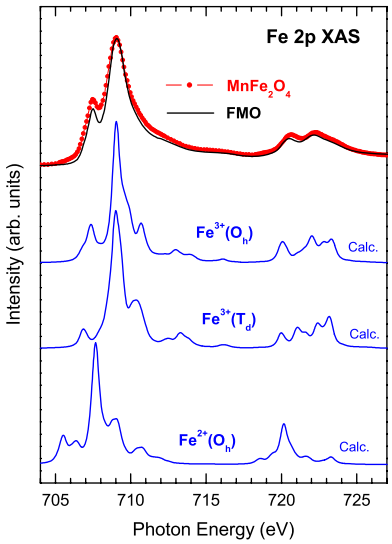

Figure 2. Comparison of the Fe 2p XAS of $(Fe,Mn)_3O_4$ to the calculated Fe 2p XAS for O_h Fe^{3+}, T_d Fe^{3+} and O_h Fe^{2+} ions.

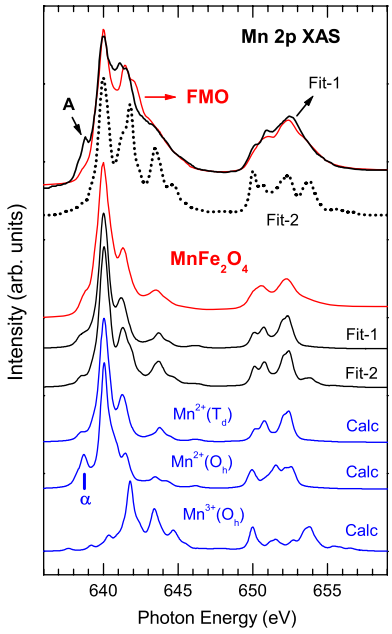

Figure 3. Comparison of the measured Mn 2p XAS spectra (red) of $(Fe,Mn)_3O_4$ to the calculated Mn 2p XAS (blue lines at the bottom) for T_d Mn_A^{2+} ($3d^5$), O_h Mn_B^{2+} ($3d^5$) and O_h Mn_B^{3+} ($3d^4$) ions, respectively. Two fitting results for FMO are shown: 'Fit-1' (black line) represents the weighted sum of the experimental XAS spectra of (45% MnO and 55% Mn_2O_3). 'Fit-2' (black dotted line) represents the weighted sum of (45% Mn_A^{2+} and 55% Mn_B^{3+}) calculations. The two fitting results for $MnFe_2O_4$, labeled as 'Fit-1' and 'Fit-2', represent the weighted sum of (80% Mn_A^{2+} and 20% Mn_B^{2+}) and (80% Mn_A^{2+} and 20% Mn_B^{3+}) calculations, respectively.

calculated Fe^{2+} states. In the quantitative aspect, however, the calculated XAS spectra are somewhat different from the measured XAS spectra of $(Fe,Mn)_3O_4$ (figure 2), as compared to the similarity among the measured XAS spectra of α-Fe_2O_3, γ-Fe_2O_3 and $(Fe,Mn)_3O_4$ (figure 1(a)). Hence we cannot tell clearly the occupation sites of Fe^{3+} ions based on the LFM

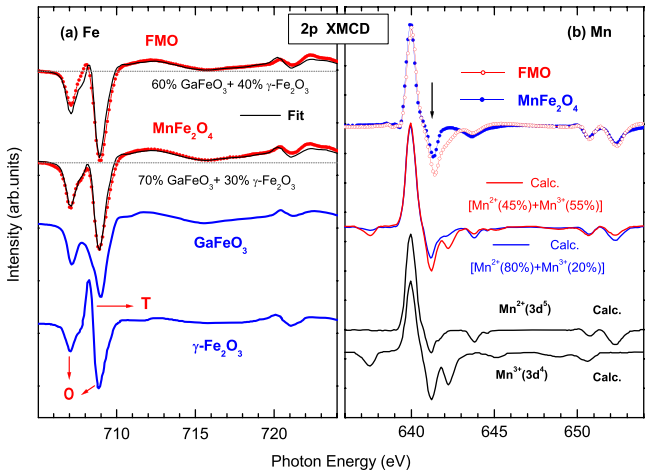

Figure 4. (a) Comparison of the Fe 2p XMCD of $(Fe,Mn)_3O_4$ to those of $GaFeO_3$ [24], γ-Fe_2O_3 [24] and their weighted sums. (b) Comparison of the measured Mn 2p XMCD of $(Fe,Mn)_3O_4$ to the calculated Mn 2p XMCD for $Mn^{2+}(3d^5)$ and $Mn^{3+}(3d^4)$ ions [29], and their weighted sums.

calculations. The determination of the occupation sites will be made in the analysis of XMCD spectra of $(Fe,Mn)_3O_4$ in figure 4.

Figure 3 compares the measured Mn 2p XAS spectra (red) of $(Fe,Mn)_3O_4$ to the LFM calculations for Mn 2p XAS. The three calculated XAS spectra at the bottom (blue lines) represent those for Mn_A^{2+} ($3d^5$; T_d), Mn_B^{2+} ($3d^5$; O_h) and Mn_B^{3+} ($3d^4$; O_h), with the crystal field energy $10Dq = 0.6$ eV, $10Dq = 1.2$ eV and $10Dq = 1.2$ eV, respectively. Two fitting results for FMO are shown: 'Fit-1' (black line) represents the weighted sum of the experimental XAS spectra of MnO (see figure 1(b)) and Mn_2O_3 (see figure 1(b)) with the ratio of [45% MnO and 55% Mn_2O_3]. 'Fit-2' (black dotted line) represents the weighted sum of [45% Mn_A^{2+} (T_d) and 55% Mn_B^{3+} (O_h)] calculations. The former fitting using the experimental data of MnO and Mn_2O_3 yields better agreement with the measured XAS of FMO than the latter fitting using the calculations. The discrepancy for feature A ($h\nu \sim 639$ eV) seems to be due to the fact that Mn ions in MnO have the O_h symmetry only. This argument is supported by the feature 'α' in the calculated XAS for Mn_B^{2+} ($3d^5$; O_h), which is absent in the calculated XAS for Mn_A^{2+} ($3d^5$; T_d). According to these fittings for FMO, we can conclude that FMO has the nearly inverse spinel configuration, corresponding to $\approx(Mn_{0.9}^{2+}Fe_{0.1}^{3+})_A[Fe_{0.8}^{3+}Mn_{1.2}^{3+}]_BO_4$ ($y \approx 0.85$).

On the other hand, for $MnFe_2O_4$, the inversion parameter $y \approx 0.2$ gives the best fitting for Mn 2p XAS. As to the fitting results of $MnFe_2O_4$, 'Fit-1' and 'Fit-2' for $MnFe_2O_4$ represent the weighted sums of (80% $Mn_A^{2+}(T_d)$ and 20% $Mn_B^{2+}(O_h)$) to describe the single-valent states of Mn ions, and (80% $Mn_A^{2+}(T_d)$ and 20% $Mn_B^{3+}(O_h)$) to describe the mixed-valent states of Mn ions, respectively. The latter fit 'Fit-2' was made in order to check the consistency between our data and the mixed-valent picture for $MnFe_2O_4$ [6, 12]. Both fits yield good agreement with experiment. Hence, at the moment, we cannot finalize whether the valence

states of Mn and Fe ions in $MnFe_2O_4$ are single-valent such as $(Mn^{2+}_{0.8}Fe^{3+}_{0.2})_A[Fe^{3+}_{1.8}Mn^{2+}_{0.2}]_BO_4$ or mixed-valent such as $(Mn^{2+}_{0.8}Fe^{3+}_{0.2})_A[Fe^{3+}_{1.6}Fe^{2+}_{0.2}Mn^{3+}_{0.2}]_BO_4$.

Figure 4(a) compares the Fe 2p XMCD spectra of $(Fe,Mn)_3O_4$ (red dots) to those of $GaFeO_3$ [24] and γ-Fe_2O_3 [24], which were obtained at the same beamline of the PAL and under the similar experimental conditions as our $(Fe,Mn)_3O_4$ data. We have shifted $GaFeO_3$ by −0.42 eV and γ-Fe_2O_3 by −0.83 eV to align their O_h peaks to those of our XMCD spectra of $(Fe,Mn)_3O_4$. The weighted sum (black line) of 60% $GaFeO_3$ and 40% γ-Fe_2O_3 is superposed upon the XMCD spectrum of FMO. Similarly, the weighted sum (black line) of 70% $GaFeO_3$ and 30% γ-Fe_2O_3 is superposed upon the XMCD spectrum of $MnFe_2O_4$. Note that the XMCD spectrum of $GaFeO_3$ has the contribution only from O_h Fe^{3+} ions [24], whereas that of γ-Fe_2O_3 has a mixture of Fe^{3+}_A (T_d) and Fe^{3+}_B (O_h) ions [26] (see the labels in figure 4). In γ-Fe_2O_3, the sign of the dichroic contribution of T_d ions to XMCD is opposite to that of O_h ions because the main magnetic coupling between O_h and T_d sites is antiferromagnetic.

Note that the Fe 2p XMCD spectra of $(Fe,Mn)_3O_4$ are described very well by a linear combination of $GaFeO_3$ and γ-Fe_2O_3 (in particular for the feature around $h\nu \sim 708$ eV), which indicates the existence of both T_d Fe^{3+}_A and O_h Fe^{3+}_B ions in $(Fe,Mn)_3O_4$. This conclusion is consistent with that of figure 1(a). Considering 100% O_h Fe^{3+} ions for $GaFeO_3$ and $Fe^{3+}_A/Fe^{3+}_B = T_d/O_h = 3/5$ for γ-Fe_2O_3, these fittings yield the estimated T_d/O_h ratio of $T_d/O_h = 0.11/0.89 \approx 0.1/0.9$ for $MnFe_2O_4$, and $T_d/O_h \approx 0.15/0.85$ for FMO, respectively. Hence, among 0.9 Fe ions in $Fe_{0.9}Mn_{2.1}O_4$, about 0.13 (≈0.1) Fe ions occupy the A(T_d) site and about 0.77 (≈0.8) Fe ions occupy the B(O_h) site. That is, one can express $Fe_{0.9}$ roughly as $\sim(Fe_{0.1})_A[Fe_{0.8}]_B$.

Figure 4(b) compares the Mn 2p XMCD spectra of $(Fe,Mn)_3O_4$ to the calculated Mn 2p XMCD spectra [29] for $Mn^{2+}(3d^5)$ and $Mn^{3+}(3d^4)$ states under the spherical symmetry, and the weighted sum of (45% Mn^{2+} and 55% Mn^{3+}) and that of (80% Mn^{2+} and 20% Mn^{3+}). These calculations describe the multiplet features of XMCD of $(Fe,Mn)_3O_4$ qualitatively well. In particular, the negative feature (marked with an arrow) around $h\nu \sim 641$ eV is larger in FMO than in $MnFe_2O_4$, providing clear evidence for the existence of Mn^{3+} states in FMO. On the other hand, both 100% Mn^{2+} calculation and the sum of (80% Mn^{2+} and 20% Mn^{3+}) calculations seem to agree with the measured Mn 2p XMCD of $MnFe_2O_4$ within the fitting uncertainty.

This study shows that, in $Fe_{0.9}Mn_{2.1}O_4$, Fe ions are mainly trivalent (3+) and that the majority of Fe ions occupy the B(O_h) sites, with about 15% of the inverted Fe^{3+}_A (T_d) ions. Mn ions are mixed-valent with approximately 45% Mn^{2+}_A and 55% Mn^{3+}_B ions. Hence formal $Fe_{0.9}Mn_{2.1}O_4$ can be written roughly as $\approx(Mn^{2+}_{0.9}Fe^{3+}_{0.1})_A[Fe^{3+}_{0.8}Mn^{3+}_{1.2}]_BO_4$, reflecting the nearly inverse spinel configuration of $y \approx 0.85$. As to $MnFe_2O_4$, Mn and Fe ions are nearly divalent (Mn^{2+}) and trivalent (Fe^{3+}), respectively, and both Mn and Fe ions have mixed configurations of T_d and O_h sites with the inversion parameter $y \approx 0.2$. Hence $MnFe_2O_4$ belongs to the nearly normal spinel. As for the valence states of $MnFe_2O_4$, our XAS and XMCD data do not show clear evidence for the mixed-valent states, and so we cannot finalize the exact valence states of $MnFe_2O_4$ at the moment. So this issue remains to be resolved.

4. Conclusions

The valence states and the occupation sites of FMO and $MnFe_2O_4$ have been investigated by employing XAS and XMCD. In FMO, Fe ions are mainly trivalent (3+) and the majority of Fe^{3+} ions occupy the B(O_h) sites, while Mn ions are mixed-valent with approximately 45% Mn^{2+}_A at the A(T_d) sites and 55% Mn^{3+}_B ions at the B(O_h) sites. Therefore the formal $Fe_{0.9}Mn_{2.1}O_4$ is identified as $\approx(Mn^{2+}_{0.9}Fe^{3+}_{0.1})_A[Fe^{3+}_{0.8}Mn^{3+}_{1.2}]_BO_4$, corresponding to the nearly inverse spinel configuration of $y \approx 0.85$. In $MnFe_2O_4$, Mn and Fe ions are mainly divalent (Mn^{2+}) and trivalent (Fe^{3+}), respectively, corresponding to the nearly normal spinel configuration with the inversion parameter $y \approx 0.2$. But our XAS/XMCD data can be described either by the single-valent states or by the mixed-valent states.

Acknowledgments

This work was supported by the KRF (KRF-2006-311-C00277), by the KOSEF (R01-2006-000-10369-0), by the KOSEF through the eSSC at POSTECH, and by the Department Specialization Fund of the CUK (2008). Work at Rutgers was supported by NSF-DMR-0405682. PAL is supported by the MOST and POSCO in Korea.

References

[1] Choi H C, Shim J H and Min B I 2006 *Phys. Rev.* B **74** 172103
[2] Noh H-J, Yeo S, Kang J-S, Zhang C L, Cheong S-W, Oh S-J and Johnson P D 2006 *Appl. Phys. Lett.* **88** 081911
[3] Zhang C L, Yeo S, Horibe Y, Choi Y J, Guha S, Croft M and Cheong S-W 2007 *Appl. Phys. Lett.* **90** 133123
[4] Goodenough J B 1976 *Magnetism and the Chemical Bond* (New York: Krieger)
[5] Baron V, Gutzmer J, Rundlöf H and Tellgren R 1998 *Am. Mineral.* **83** 786
[6] Harrison F W, Osmond W P and Teale R W 1957 *Phys. Rev.* **106** 865
[7] Boucher B, Buhl R and Perrin M 1969 *J. Appl. Phys.* **40** 1126
[8] Sawatzky G A, van der Woode F and Morrish A H 1969 *Phys. Rev.* **187** 747
[9] Šimša Z and Brabers V A M 1975 *IEEE. Trans. Magn.* **11** 1303
[10] Stichauer L *et al* 2001 *J. Appl. Phys.* **90** 2511
[11] de Medeiros S N, Luciano A, Cotica L F, Santos I A, Paesano A Jr and da Cunha J B M 2004 *J. Magn. Magn. Mater.* **281** 227
[12] Shim J H, Lee S and Min B I 2007 *Phys. Rev.* B **75** 134406
[13] Noh H-J *et al* 2007 *Europhys. Lett.* **78** 27004
[14] Kubo T, Hirai A and Abe H 1969 *J. Phys. Soc. Japan* **26** 1094
[15] Shirakashi T and Kubo T 1979 *Am. Mineral.* **64** 599
[16] de Groot F M F, Fuggle J C, Thole B T and Sawatzky G A 1990 *Phys. Rev.* B **42** 5459
[17] van der Laan G and Kirkman I W 1992 *J. Phys.: Condens. Matter* **4** 4189
[18] Wi S C *et al* 2004 *Appl. Phys. Lett.* **84** 4233
[19] Thole B T, Carra P, Sette F and van der Laan G 1992 *Phys. Rev. Lett.* **68** 1943

[20] Chen C T, Idzerda Y U, Lin H-J, Smith N V, Meigs G, Chaban E, Ho G H, Pellegrin E and Sette F 1995 *Phys. Rev. Lett.* **75** 152
[21] Han S W *et al* 2006 *J. Phys.: Condens. Matter* **18** 7413
[22] Singh D J, Gupta M and Gupta R 2002 *Phys. Rev.* B **65** 064432
[23] Zhang C L *et al* 2008 unpublished
[24] Kim J-Y, Koo T Y and Park J-H 2006 *Phys. Rev. Lett.* **96** 047205
[25] Regan T J, Ohldag H, Stamm C, Nolting F, Lüning J, Stöhr J and White R L 2001 *Phys. Rev.* B **64** 214422
[26] Brice-Profeta S, Arrio M-A, Tronc E, Menguy N, Letard I, Cartier dit Moulin C, Nogues M, Chaneac C, Jolivet J-P and Sainctavit Ph 2005 *J. Magn. Magn. Mater.* **288** 354
[27] Mitra C, Hu Z, Raychaudhuri P, Wirth S, Csiszar S I, Hsieh H H, Lin H-J, Chen C T and Tjeng L H 2003 *Phys. Rev.* B **67** 92404
[28] Ghigna P, Campana A, Lascialfari A, Caneschi A, Gatteschi D, Tagliaferri A and Borgatti F 2001 *Phys. Rev.* B **64** 132413
[29] van der Laan G and Thole B T 1991 *Phys. Rev.* B **43** 13401